

CONVEXIFICATION FOR A 1D HYPERBOLIC COEFFICIENT INVERSE PROBLEM WITH SINGLE MEASUREMENT DATA

ALEXEY SMIRNOV

MICHAEL KLIBANOV* AND LOC NGUYEN

Department of Mathematics and Statistics
University of North Carolina Charlotte
Charlotte, NC 28223, USA

(Communicated by the associate editor name)

ABSTRACT. A version of the convexification numerical method for a Coefficient Inverse Problem for a 1D hyperbolic PDE is presented. The data for this problem are generated by a single measurement event. This method converges globally. The most important element of the construction is the presence of the Carleman Weight Function in a weighted Tikhonov-like functional. This functional is strictly convex on a certain bounded set in a Hilbert space, and the diameter of this set is an arbitrary positive number. The global convergence of the gradient projection method is established. Computational results demonstrate a good performance of the numerical method for noisy data.

1. Introduction. We call a numerical method for a Coefficient Inverse Problem (CIP) *globally convergent* if there exists a theorem claiming that this method delivers at least one point in a sufficiently small neighborhood of the exact solution without an assumption that the starting point of iterations is located sufficiently close to that solution. We construct in this paper a globally convergent numerical method for a CIP for a 1D hyperbolic PDE. This CIP has a direct application in standoff imaging of dielectric constants of explosive-like targets using experimentally collected data. Our numerical method is a version of the so-called *convexification* concept. Just as in all previous publications about the convexification, which are cited below, we work with the data resulting from a single measurement event. Thus, our data depend on one variable.

The reason of our work on the convexification method is the well known fact that conventional Tikhonov least squares cost functionals for CIPs suffer from the phenomenon of multiple local minima and ravines, see, e.g. the work of Scales, Fischer and Smith [35] for a convincing numerical example of this phenomenon. On the other hand, any version of the gradient method of the minimization of that functional stops at any local minimum. Therefore, a numerical reconstruction technique, which is based on the minimization of that functional, is unreliable.

The convexification method for our particular CIP was not constructed in the past. Thus, we develop some new ideas here. The first new idea is to apply certain new changes of

2010 *Mathematics Subject Classification.* Primary: 35R30; Secondary: 35L10.

Key words and phrases. 1D hyperbolic equation, coefficient inverse problem, globally convergent method, convexification, Carleman estimate.

The work was supported by US Army Research Laboratory and US Army Research Office grant W911NF-19-1-0044.

* Corresponding author: Michael Klibanov (mklibanv@uncc.edu).

variables to the original problem to obtain a new Cauchy problem with the lateral Cauchy data for a quasilinear integro-differential equation with Volterra-like integrals in it. As soon as the solution of this problem is obtained, the target unknown coefficient can be computed by a simple backwards calculation. The second new idea is to obtain a new Carleman estimate for the principal part of the operator of that equation (Theorem 4.1). The Carleman Weight Function (CWF) in that estimate is also new. A surprising and newly observed property of that Carleman estimate is that a certain resulting integral, the one over an interval of a certain straight line, is non-negative. It is this property, which, in combination with the rest of that Carleman estimate, enables us to construct the *key element* of the convexification, a globally strictly convex cost functional with the above mentioned CWF in it and then to prove the global convergence of our numerical method (Theorems 4.2-4.6). Since such a functional was not constructed for our CIP in the past, then both this construction and follow up Theorems 4.2-4.6 are also new.

Below $x \in \mathbb{R}$, $t > 0$. Let the function $a(x) \in C^1(\mathbb{R})$ possesses the following properties:

$$a(x) \geq 0 \quad \text{for } x \in (0, 1), \quad (1.1)$$

$$a(x) = 0 \quad \text{for } x \notin (0, 1). \quad (1.2)$$

Problem. (*Forward Problem.*) *The forward problem we consider here is the problem of the search of the fundamental solution $u(x, t)$ of the hyperbolic operator $\partial_t^2 - \partial_x^2 - a(x)$, with $a(x)$ satisfying (1.1), (1.2) i.e.*

$$\begin{cases} u_{tt} = u_{xx} + a(x)u, & (x, t) \in \mathbb{R} \times (0, \infty), \\ u(x, 0) = 0, & u_t(x, 0) = \delta(x), \end{cases} \quad (1.3)$$

where $\delta(x)$ is the Dirac function at $x = 0$.

Problem. (*Coefficient Inverse Problem.*) Determine the coefficient $a(x)$ satisfying conditions (1.1), (1.2), assuming that the following two functions $f_0(t), f_1(t)$ are given:

$$u(0, t) = f_0(t), \quad u_x(0, t) = f_1(t), \quad \forall t \in (0, T), \quad (1.4)$$

where the number $T > 0$ will be defined later.

It is the CIP (1.3), (1.4) for which we develop here the convexification method. It is well known that, given (1.2), functions $f_0(t), f_1(t)$ for $t \in (0, 2)$ (i.e. for $T = 2$) uniquely determine the function $a(x)$ and also the Lipschitz stability estimate holds, see Theorem 2.6 Section 3 of Chapter 2 of [34] as well as Figure 1(B).

As to the Dirac function in the initial condition (1.3), this function is an idealization of the reality of course. Therefore, its approximation is used in real world problems of physics. Nevertheless, the Dirac function is commonly used in many applied problems to model an ultra-short pulse, that penetrates deeply lossy materials and allows one to achieve very fine imaging resolution. An ultra-short pulse system is attractive for applications, due to its low power spectral density that results in negligible interference with other signals. There are various techniques to generate short pulses in the order of nanoseconds. In this regard, we refer to, e.g. an applied paper [1], where a short pulse is approximated via a narrow Gaussian. It is well known that such a function approximates the Dirac function in a certain sense. Another confirmation of the usefulness of the modeling via the Dirac function comes from [24], where this function was successfully used to work with some experimental data via a version of the convexification method for a 1D CIP in the frequency domain.

To describe some applications of our CIP, we briefly consider here a similar inverse problem for the 1D acoustic equation,

$$\begin{cases} U_{tt} = c^2(y)U_{yy}, & (y,t) \in \mathbb{R} \times (0, \infty), \\ U(y,0) = 0, & U_t(y,0) = \delta(y). \end{cases} \quad (1.5)$$

where the sound speed $c(y) \in C^3(\mathbb{R})$ is such that $c(y) \geq c_0 = \text{const} > 0$ and $c(y) = 1$ for $y \in \{(-\infty, 0) \cup (1, \infty)\}$. The coefficient inverse problem in this case consists of determining the function $c(y)$ for $y \in (0, 1)$, given functions $g_0(t)$ and $g_1(t)$,

$$U(0,t) = g_0(t), U_y(0,t) = g_1(t), \quad t \in (0, T'), \quad (1.6)$$

where the number $T' = T'(T)$ depends on T in (1.4).

We start by applying a widely known change of variables, see e.g. [34]:

$$x \leftrightarrow y \quad \Rightarrow \quad x(y) = \int_0^y \frac{ds}{c(s)}$$

Then $x(y)$ is the travel time of the acoustic signal from the point $\{0\}$ to the point $\{y\}$. Next, we introduce a new function $V(x,t) = U(y(x),t)/S(x)$, where $S(x) = \sqrt{c(y(x))}$. Then problem (1.5)-(1.6) becomes

$$\begin{cases} V_{tt} = V_{xx} + p(x)V, & (x,t) \in \mathbb{R} \times (0, \infty), \\ V(x,0) = 0, & V_t(x,0) = \delta(x), \\ V(0,t) = g_0(t), & V_x(0,t) = g_1(t), \quad t \in (0, T), \end{cases} \quad (1.7)$$

where

$$p(x) = \frac{S''(x)}{S(x)} - 2 \left[\frac{S'(x)}{S(x)} \right]^2 = \frac{1}{2} c''(y(x))c(y(x)) - \frac{1}{4} [c'(y(x))]^2.$$

Equations (1.7) look exactly as equations (1.3)-(1.4). Hence, we have reduced the CIP (1.5)-(1.6) to our CIP (1.3)-(1.4). This justifies the applied aspect of our CIP. On the other hand, due to the presence of the unknown coefficient $c(y)$ in the principal part of the hyperbolic operator of (1.5), the CIP (1.5)-(1.6) is harder to work with than the CIP (1.3)-(1.4). Therefore, it makes sense, as the first step, to develop a numerical method for the CIP (1.3)-(1.4). Next, one might adapt that technique to problem (1.5)-(1.6). This first step is done in the current paper.

The CIP (1.5)-(1.6) has application in acoustics [8]. Another quite interesting application is in inverse scattering of electromagnetic waves, in which case $c^{-2}(y) = \varepsilon_r(y)$, where $\varepsilon_r(y)$ is the spatially distributed dielectric constant. Using the data, which were experimentally collected by the US Army Research Laboratory, it was demonstrated in [14, 24, 32] that the 1D mathematical model, which is based on equation (1.5), can be quite effectively used to image in the standoff mode dielectric constants of targets, which mimic explosives, such as, e.g. antipersonnel land mines and improvised explosive devices. In fact, the original data in [14, 24, 32] were collected in the time domain. However, the mathematical apparatus of these references works only either with the Laplace transform [14, 32] or with the Fourier transform [24] with respect to t of equation (1.5). Unlike these, we hope that an appropriately modified technique of the current paper should help us in the future to work with those experimental data directly in the time domain.

Of course, the knowledge of the dielectric constant alone is insufficient to differentiate between explosives and non-explosives. However, we believe that this knowledge might be used in the future as an ingredient, which would be an additional one to the currently existing features which are used in the classification procedures for such targets. So that

this additional ingredient would decrease the current false alarm rate, see, e.g. page 33 of [32] for a similar conclusion. As to other globally convergent numerical methods for the 1D CIPs for the wave-like equations, we refer to works of Korpela, Lassas and Oksanen [29, 30], where a CIP for equation (1.5) is studied without the above change of variables. The data of [29, 30] depend on two variables since those are the Neumann-to-Dirichlet data. We also refer to the works of Kabanikhin with coauthors. First, this group has computationally implemented in the 1D case [13] the Gelfand-Krein-Levitan method (GKL) [10, 31]. Next, they have extended the GKL method to the 2D case and studied that extension computationally, see, e.g. [13, 11, 12]. In the original 1D version of GKL [10, 31], one reduces an analog of our CIP to a Fredholm-type linear integral equation of the second kind. The data for the CIP form the kernel of this equation. The solution of this equation provides one with the target unknown coefficient. In the 2D version of GKL, one obtains a system of coupled Fredholm-type linear integral equations of the second kind. The solution of this system allows one to calculate the unknown coefficient.

At the same time, it was demonstrated numerically in [14] that while GKL works well for computationally simulated data in the 1D case, it fails to perform well for experimentally collected data. The latter is true at least for the experimental data of [14]. These are the same experimental data as ones in [24, 32]. This set of data is particularly important to us, since it is about the main application of our interest: imaging of dielectric constants of explosive-like targets. On the other hand, it was demonstrated in [24] that another 1D version of the convexification method performs well for the same experimental data. The version of [24] works with the data in the frequency domain, while the current paper works with the data in the time domain. We are not working with those experimental data in this paper, since such an effort would require a substantial investment of time from us, and we simply do not have this time at this moment. However, as stated above, in the future we indeed plan to apply the technique of the current paper to the experimental data of [14, 24, 32]. Thus, we point out that while results of [24] show a good promise in this direction for the version of the convexification of the current paper, results of [14] tell us that GKL is likely not applicable to those experimental data.

In the 2D case, the GKL uses overdetermined data [13, 11, 12]. This means that the 2D version of GKL requires that the number $m = 3$ of free variables in the data would exceed the number $n = 2$ of free variables in the unknown coefficient, i.e. $m > n$. On the other hand, in all publications about the convexification, which we cite below, so as in this one, the data are non overdetermined, i.e. $m = n$. In particular, in this paper $m = n = 1$.

Being motivated by the goal of avoiding the above mentioned phenomenon of multiple local minima and ravines of conventional least squares Tikhonov functionals, Klibanov with coauthors has been working on the convexification since 1995, see [5, 21, 19, 22] for the initial works on this topic. The publication of Bakushinskii, Klibanov and Koshev [2] has addressed some questions, which were important for the numerical implementation of the convexification. This has opened the door for some follow up publications about the convexification, including the current one, with a variety of computational results [16, 15, 24, 27, 26, 24, 28]. We also refer to the works of Baudouin, De Buhan and Ervedoza and Osses [3, 4], where a different version of the convexification is developed for two n -D CIPs ($n = 1, 2, \dots$) for the hyperbolic equations. Both versions of the convexification mentioned in this paragraph use the idea of the Bukhgeim-Klibanov method [7].

As to the Bukhgeim-Klibanov method, it was originated in [7] with the only goal at that time (1981) of proofs of global uniqueness theorems for multidimensional CIPs with single measurement data. This method is based on Carleman estimates. The convexification extends the idea of [7] from the initial purely uniqueness topic to the more applied topic of

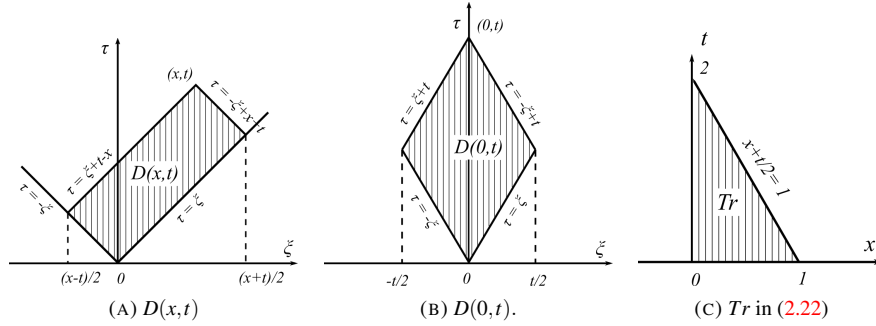


FIGURE 1. The rectangle $D(x,t) = \{(\xi, \tau) : |\xi| < \tau < t - |x - \xi|\}$ and the triangle Tr .

numerical methods for CIPs. Many publications of many authors are devoted to the method of [7] being applied to a variety of CIPs, again with the goals of proofs of uniqueness and stability results for those CIPs. Since the current paper is not a survey of that technique, we now refer only to a few of such publications [6, 17, 18, 20].

All functions below are real valued ones. In Section 2 we derive a boundary value problem for a quasilinear integro-differential equation. In Section 3 we describe the convexification method for solving this problem. We formulate our theorems in Section 4. Their proofs are in Section 5. Numerical results are presented in Section 6.

2. Quasilinear Integro-Differential Equation. Let $H(x)$ be the Heaviside function centered at $x = 0$. Problem (1.3) is equivalent to the following integral equation, see Section 3 of Chapter 2 of [34]:

$$u(x,t) = \begin{cases} \frac{1}{2}H(t - |x|) + \frac{1}{2} \int_{D(x,t)} a(\xi) u(\xi, \tau) d\xi d\tau, & \text{for } t > |x|, \\ 0, & \text{for } 0 < t < |x|. \end{cases} \quad (2.1)$$

$$D(x,t) = \{(\xi, \tau) : |\xi| < \tau < t - |x - \xi|\}. \quad (2.2)$$

It follows from (2.2) and (1.2) that the first line of (2.1) can be rewritten as [34]:

$$u(x,t) = \frac{1}{2}H(t - |x|) + \frac{1}{2} \int_0^{(x+t)/2} a(\xi) \int_{|\xi|}^{t-|x-\xi|} u(\xi, \tau) d\tau d\xi. \quad (2.3)$$

see Figure 1. In fact, (2.3) is a linear integral equation of the Volterra type with respect to the function $u(x,t)$ [34]. This equation can be solved as:

$$u_0(x,t) = \frac{1}{2}H(t - |x|), \quad u_n(x,t) = \frac{1}{2} \int_0^{(x+t)/2} a(\xi) \int_{|\xi|}^{t-|x-\xi|} u_{n-1}(\xi, \tau) d\tau d\xi \quad (2.4)$$

$$u(x,t) = \sum_{n=0}^{\infty} u_n(x,t), \quad |u_n(x,t)| \leq \frac{(Mt)^n}{n!}, \quad x \in (\alpha_1, \alpha_2), \quad (2.5)$$

for $n = 1, 2, \dots$ and for any finite interval $(\alpha_1, \alpha_2) \subset \mathbb{R}$, where the number $M = M(\alpha_1, \alpha_2, \|a\|_{C[0,1]}) > 0$ depends only on the listed parameters. Similar estimates can

be obtained for derivatives $\partial_x^k \partial_t^s u_n$ with $k + s \leq 3$, except that in this case $M = M(\alpha_1, \alpha_2, \|a\|_{C^1[0,1]}) > 0$. We also note that since by (1.1) $a(x) \geq 0$, then (2.4)-(2.5) imply that

$$u(x, t) \geq \frac{1}{2} \text{ for } t \geq |x|. \quad (2.6)$$

Thus, (2.1)-(2.6) imply that the following lemma is valid [34]:

Lemma 2.1. There exists a unique solution $u(x, t)$ of problem (2.1) such that $(u - u_0)(x, t) \in C\{t \geq 0\}$, $u(x, t) \in C^3\{(x, t) \mid t \geq |x|\}$. Problem (2.1) is equivalent to the Cauchy problem (1.3)-(1.4). Furthermore, $\lim_{t \rightarrow |x|^+} u(x, t) = 1/2$ and inequality (2.6) holds.

2.1. Integro-differential equation. Consider the function $u(x, t)$ for $x > 0$ above the characteristic cone $\{t = |x|\}$ and change the variables as

$$v(x, t) = u(x, t + x), \text{ for } x, t > 0. \quad (2.7)$$

Then (1.3), (1.4), (2.6) and Lemma 2.1 imply that

$$v_{xx} - 2v_{xt} + a(x)v = 0, \text{ for } x, t > 0, \quad (2.8)$$

$$v(x, 0) = \frac{1}{2}, \text{ for } x > 0, \quad (2.9)$$

$$v(0, t) = f_0(t), v_x(0, t) = f_0'(t) + f_1(t). \quad (2.10)$$

In addition, (2.6) and (2.7) imply that

$$v(x, t) \geq \frac{1}{2}, \text{ for } x, t > 0. \quad (2.11)$$

It follows from (2.11) that we can consider the function

$$q(x, t) = \ln v(x, t). \quad (2.12)$$

Using (2.8)-(2.10), we obtain

$$q_{xx} - 2q_{xt} + q_x^2 - 2q_x q_t = -a(x), \text{ for } x, t > 0, \quad (2.13)$$

$$q(x, t) = -\ln 2, \quad (2.14)$$

$$q(0, t) = \ln f_0(t), \quad q_x(0, t) = \frac{f_0'(t) + f_1(t)}{f_0(t)}. \quad (2.15)$$

Equation (2.13) has two unknown functions, $q(x, t)$ and $a(x)$, which is inconvenient. On the other hand, the function $a(x)$ is “isolated” in (2.13) and it is independent on t . Therefore, we follow the first step of the method of [7]. More precisely, we differentiate both sides of equation (2.13) with respect to t . Thus, we eliminate the unknown coefficient from this equation and obtain an integro-differential equation this way.

Let

$$w(x, t) = q_t(x, t). \quad (2.16)$$

Then (2.14) and (2.16) imply

$$q(x, t) = \int_0^t w(x, \tau) d\tau - \ln 2. \quad (2.17)$$

Define the quasilinear integro-differential operator L as

$$L(w) = w_{xx} - 2w_{xt} + 2w_x \int_0^t w_x(x, \tau) d\tau - 2w_x w - 2w_t \int_0^t w_x(x, \tau) d\tau. \quad (2.18)$$

Hence, (2.13)-(2.18) imply

$$L(w) = 0, \quad (x, t) \in Tr, \quad (2.19)$$

$$w(0, t) = p_0(t), \quad w_x(0, t) = p_1(t), \quad (2.20)$$

where

$$p_0(t) = f_0'(t)/f_0(t), \quad p_1(t) = \frac{d}{dt}[(f_0'(t) + f_1(t))/f_0(t)]. \quad (2.21)$$

As to the domain Tr in (2.19), it is clear that the change of variables (2.7) transforms the rectangle $D(0, t)$ of Figure 1(B) in the triangle Tr , see Figure 1(C),

$$Tr = \left\{ (x, t) : x, t > 0, x + \frac{t}{2} < 1 \right\}. \quad (2.22)$$

Hence, we can uniquely determine the functions $w(x, t)$ and $q(x, t)$ only for $(x, t) \in Tr$.

2.2. Absorbing boundary conditions.

Lemma 2.2. For every two numbers $A \geq 1$ and $B > 0$, the function $u(x, t)$ satisfies the absorbing boundary conditions:

$$u_x(A, t) + u_t(A, t) = 0, \quad u_x(-B, t) - u_t(-B, t) = 0, \quad \forall t \in (0, T).$$

Proof. Clearly the function $u_0(x, t)$ defined in (2.4) satisfies these conditions. Denote $\tilde{u}(x, t) = u(x, t) - u_0(x, t)$. Differentiating (2.3), we obtain

$$\begin{aligned} \tilde{u}_x(x, t) &= -\frac{1}{2} \int_0^{(x+t)/2} \operatorname{sgn}(x - \xi) a(\xi) u(\xi, t - |x - \xi|) d\xi, \\ \tilde{u}_t(x, t) &= \frac{1}{2} \int_0^{(x+t)/2} a(\xi) u(\xi, t - |x - \xi|) d\xi. \end{aligned} \quad (2.23)$$

If $x \geq 1$, then in (2.23) $\operatorname{sgn}(x - \xi) = 1$, since $a(\xi) = 0$ for $\xi \geq 1$. Next, if $x \leq 0$, then in (2.23) $\operatorname{sgn}(x - \xi) = -1$ since $a(\xi) = 0$ for $\xi \leq 0$. \square

Remark 1. Engquist and Majda have proposed to impose the absorbing boundary conditions for the numerical simulations of the propagation of waves [9]. Lemma 2.2 implies that, unlike [9], in the case of problem (1.3), this condition should not be imposed, since it holds automatically.

Remark 2. We impose the non-negativity condition (1.1) on the unknown coefficient $a(x)$ to ensure (2.6). It is inequality (2.6), which allows us to consider the function $q(x, t) = \ln v(x, t)$ in (2.12): since (2.6) guarantees (2.11). Assumption (1.2) is important for the validity of Lemma 2.2. This lemma, in turn is quite helpful numerically for the solution of the forward problem of data simulations as well as to ensure a good stability of our inverse algorithm, see section 6. Finally, the smoothness condition $a \in C^1(\mathbb{R})$ ensures that the function $q \in C^3(x \geq 0, t \geq 0)$: see Lemma 2.1, (2.16) and (2.18). We point out that we are not looking for minimal requirements imposed on $a(x)$.

Thus, (1.2) and Lemma 2.2 imply that for any two numbers $A \geq 1, B > 0$

$$u_{tt} = u_{xx} + a(x)u, \quad (x, t) \in (-B, A) \times (0, \infty), \quad (2.24)$$

$$u(x, 0) = 0, u_t(x, 0) = \delta(x), \quad (2.25)$$

$$u_x(-B, t) - u_t(-B, t) = 0, u_x(A, t) + u_t(A, t) = 0. \quad (2.26)$$

2.3. Reconstruction of the unknown coefficient. It follows from (2.13), (2.14) and (2.16) that

$$a(x) = 2w_x(x, 0). \quad (2.27)$$

Hence, we focus below on the numerical solution of the boundary value problem (2.19), (2.21).

3. Convexification.

3.1. Convexification in brief. Given a CIP, the first step of the convexification follows the first step of [7], in which the unknown coefficient is eliminated from the PDE via the differentiation with respect to such a parameter from which that coefficient does not depend. In particular, in our case, we have replaced equation (2.13), which contains the unknown coefficient $a(x)$, with a quasilinear integro-differential equation (2.19), which does not contain that coefficient. Next, one should solve the corresponding boundary value problem, which is similar with the problem (2.19), (2.20). To solve that boundary value problem, a weighted Tikhonov-like functional J_λ is constructed, where $\lambda \geq 1$ is a parameter. The weight is the Carleman Weight Function (CWF), which is involved in the Carleman estimate for the principal part of the operator of that integro-differential equation. In our case, that principal part is the operator $\partial_x^2 - 2\partial_x\partial_t$, see (2.18) and (2.19).

The above mentioned functional is minimized on a convex bounded set with the diameter $2d$, where $d > 0$ is an arbitrary number. This set is a part of a Hilbert space H^k . In our case, $k = 3$. The key theorem is that one can choose a sufficiently large value $\tilde{\lambda}(d) \geq 1$ of the parameter λ such that the functional J_λ is strictly convex on that set for all $\lambda \geq \tilde{\lambda}$. Next, one proves that, for these values of λ , the gradient projection method of the minimization of the functional J_λ converges to the correct solution of that CIP starting from an arbitrary point of the above mentioned set, as long as the level of the noise in the data tends to zero. Given that the diameter $2d$ of that set is an arbitrary number and that the starting point is also an arbitrary one, this is the *global convergence*, by the definition of the first sentence of Introduction.

It is worth to note that even though the theory says that the parameter λ should be sufficiently large, our rich computational experience tells us that computations are far less pessimistic than the theory is. More precisely, in all our numerically oriented publications on the convexification, including the current one, accurate numerical results are obtained for $\lambda \in [1, 3]$, see [2, 16, 23, 26, 27, 25, 24].

3.2. The Tikhonov-like functional with the Carleman Weight Function in it. We construct this functional to solve problem (2.19), (2.20). Everywhere below $\alpha \in (0, 1/2)$. Our CWF has the form:

$$\varphi_\lambda(x, t) = \exp(-2\lambda(x + \alpha t)), \quad (3.1)$$

where $\lambda \geq 1$ is a parameter, see Theorem 4.1 in section 4 for the Carleman estimate with this CWF. Even though we can find the function $w(x, t)$ only in the triangle Tr in (2.22), it is convenient for our numerical study to work with the rectangle R ,

$$R = (0, 1) \times (0, T), \quad T \geq 2. \quad (3.2)$$

Using (2.7), (2.12), (2.16) and the absorbing boundary condition (2.26) for $A = 1$, we obtain

$$w_x(1, t) = 0. \quad (3.3)$$

Let $d > 0$ be an arbitrary number. Define the set $B(d, p_0, p_1)$ as

$$B(d, p_0, p_1) = \left\{ w \in H^3(R) : w(0, t) = p_0(t), w_x(0, t) = p_1(t), w_x(1, t) = 0, \|w\|_{H^3(R)} < d \right\}. \quad (3.4)$$

Let $\beta \in (0, 1)$ be the regularization parameter and $L(w)$ be the operator defined in (2.18). Our weighted Tikhonov-like functional is:

$$J_{\lambda, \beta}(w) = \int_R [L(w)]^2 \varphi_\lambda dxdt + \beta \|w\|_{H^3(R)}^2. \quad (3.5)$$

Minimization Problem. *Minimize the functional $J_{\lambda, \beta}(w)$ on the set $B(d, p_0, p_1)$.*

3.3. Estimating an integral. We use Lemma 3.1 in the proof of Theorem 4.2 (section 4). The presence of the multiplier $1/\lambda^2$ in the right hand side of (3.6) is new since the CWF is new here. Indeed, while in (3.1) t is used, usually one uses t^2 in CWFs for similar problems, see e.g. [6, 20]. The latter implies that the term $1/\lambda$ rather than $1/\lambda^2$ is present in an analogous estimate of Lemma 1.10.3 of [6] and of Lemma 3.1 of [20]. Since these and similar lemmata are usually used in the Bukhgeim-Klibanov method and since any Carleman estimate requires that its parameter $\lambda \geq 1$ be sufficiently large, then the estimate of Lemma 3.1 is stronger than the one of [6, 20]. The proof of this estimate is also different from the one of [6, 20]. Even though we use an arbitrary $\alpha > 0$ in Lemma 3.1, still everywhere after this lemma $\alpha \in (0, 1/2)$: just as above.

Lemma 3.1. *For any two numbers $\lambda, \alpha > 0$ and for any function $g \in L^2(R)$ the following estimate is valid:*

$$\int_R \left(\int_0^t g(x, \tau) d\tau \right)^2 \varphi_\lambda dxdt \leq \frac{1}{\lambda^2 \alpha^2} \int_R g^2 \varphi_\lambda dxdt. \quad (3.6)$$

Proof. Using (3.1), integration by parts and the Cauchy-Schwarz inequality, we obtain

$$\begin{aligned}
I &= \int_R \left(\int_0^t g(x, \tau) d\tau \right)^2 \varphi_\lambda dx dt = \int_0^1 e^{-2\lambda x} \int_0^T e^{-2\lambda \alpha t} \left(\int_0^t g(x, \tau) d\tau \right)^2 dt dx = \\
& \int_0^1 e^{-2\lambda x} \int_0^T \frac{d}{dt} \left(-\frac{e^{-2\lambda \alpha t}}{2\lambda \alpha} \right) \left(\int_0^t g(x, \tau) d\tau \right)^2 dt dx = \\
& - \int_0^1 e^{-2\lambda x} \frac{e^{-2\lambda \alpha T}}{2\lambda \alpha} \left(\int_0^T g(x, \tau) d\tau \right)^2 dx \\
& + \frac{1}{\lambda \alpha} \int_R e^{-2\lambda x} e^{-2\lambda \alpha t} g(x, t) \left(\int_0^t g(x, \tau) d\tau \right) dt dx \leq \\
& \frac{1}{\lambda \alpha} \left[\int_R g^2 \varphi_\lambda dx dt \right]^{1/2} \left[\int_R \left(\int_0^t g(x, \tau) d\tau \right)^2 \varphi_\lambda dx dt \right]^{1/2}.
\end{aligned}$$

Here, we have used the fact that the term in the third line of the above is negative. Hence, we have obtained that

$$I \leq \frac{1}{\lambda \alpha} \left(\int_R g^2 \varphi_\lambda dx dt \right)^{1/2} \sqrt{I}. \quad (3.7)$$

Dividing both sides of (3.7) by \sqrt{I} and squaring both sides of the resulting inequality, we obtain (3.6). \square

4. Theorems. Introduce the subspaces $H_0^2(R) \subset H^2(R)$ and $H_0^3(R) \subset H^3(R)$,

$$H_0^2(R) = \{u \in H^2(R) : u(0, t) = u_x(0, t)\}, \quad H_0^3(R) = H^3(R) \cap H_0^2(R).$$

Theorem 4.1. (*Carleman estimate*). There exist constants $C = C(\alpha) > 0$ and $\lambda_0 = \lambda_0(\alpha) \geq 1$ depending only on α such that for all functions $u \in H_0^2(R)$ and for all $\lambda \geq \lambda_0$ the following Carleman estimate is valid:

$$\begin{aligned}
& \int_R (u_{xx} - 2u_{xt})^2 \varphi_\lambda dx dt \geq C\lambda \int_R (u_x^2 + u_t^2) \varphi_\lambda dx dt + C\lambda^3 \int_R u^2 \varphi_\lambda dx dt \\
& + C\lambda \int_0^1 u_x^2(x, 0) e^{-2\lambda x} dx + C\lambda^3 \int_0^1 u^2(x, 0) e^{-2\lambda x} dx - C\lambda e^{-2\lambda \alpha T} \int_0^1 u_x^2(x, T) dx \\
& - C\lambda^3 e^{-2\lambda \alpha T} \int_0^1 u^2(x, T) dx.
\end{aligned} \quad (4.1)$$

Remark 3. *This Carleman estimate is new. The positivity of the first two terms in the second line of (4.1) is surprising. Indeed, in Carleman estimates, usually one cannot ensure signs of integrals over hypersurfaces. In particular, using (2.27), it is shown below that the positivity of these two terms is quite helpful in the reconstruction of the unknown coefficient $a(x)$.*

Choose an arbitrary number $\varepsilon \in (0, 2\alpha)$. Consider the triangle $Tr_{\alpha, \varepsilon}$

$$Tr_{\alpha, \varepsilon} = \{(x, t) : x + \alpha t < 2\alpha - \varepsilon; \quad x, t > 0\} \subset Tr \quad (4.2)$$

Theorem 4.2. (*global strict convexity*). For an arbitrary number $d > 0$, let $B(d, p_0, p_1) \subset H^3(R)$ be the set defined in (3.4). For any $\lambda, \beta > 0$ and for any $w \in \overline{B(d, p_0, p_1)}$ the functional $J_{\lambda, \beta}(w)$ in (3.5) has the Fréchet derivative $J'_{\lambda, \beta}(w) \in H_0^3(R)$. Let $\lambda_0 = \lambda_0(\alpha) \geq 1$ be the number of Theorem 4.1. Then there exist a sufficiently large number $\lambda_1 = \lambda_1(\alpha, \varepsilon, d) \geq \lambda_0$ and a number $C_1 = C_1(\alpha, \varepsilon, d) > 0$, both depending only on listed parameters, such that for all $\lambda \geq \lambda_1$ and for all $\beta \in [2e^{-\lambda\alpha T}, 1)$, functional (3.5) is strictly convex on the set $\overline{B(d, p_0, p_1)}$. More precisely, the following inequality holds:

$$\begin{aligned} J_{\lambda, \beta}(w_2) - J_{\lambda, \beta}(w_1) - J'_{\lambda, \beta}(w_1)(w_2 - w_1) &\geq C_1 e^{-2\lambda(2\alpha - \varepsilon)} \|w_2 - w_1\|_{H^1(Tr_{\alpha, \varepsilon})}^2 \\ &+ C_1 e^{-2\lambda(2\alpha - \varepsilon)} \|w_2(x, 0) - w_1(x, 0)\|_{H^1(0, 2\alpha - \varepsilon)}^2 + \frac{\beta}{2} \|w_2 - w_1\|_{H^3(R)}^2, \quad (4.3) \\ &\forall w_1, w_2 \in \overline{B(d, p_0, p_1)}, \quad \forall \lambda \geq \lambda_1. \end{aligned}$$

Remark 4. Below $C_1 = C_1(\alpha, \varepsilon, d) > 0$ denotes different numbers depending only on listed parameters. It follows from Lemma 3 on page 9 of the book of Polyak [33] that (4.3) guarantees the strict convexity of the functional $J_{\lambda, \beta}$ on the set $\overline{B(d, p_0, p_1)}$.

Theorem 4.3. Let parameters $\lambda_1, \lambda, \beta$ be the same as in Theorem 4.2. Then there exists a unique minimizer $w_{\min, \lambda, \beta} \in \overline{B(d, p_0, p_1)}$ of the functional $J_{\lambda, \beta}(w)$ on the set $\overline{B(d, p_0, p_1)}$. Furthermore, the following inequality holds

$$J'_{\lambda, \beta}(w_{\min, \lambda, \beta})(w - w_{\min, \lambda, \beta}) \geq 0, \quad \forall w \in \overline{B(d, p_0, p_1)}. \quad (4.4)$$

To estimate the reconstruction accuracy as well as to introduce the gradient projection method, we need to obtain zero Dirichlet and Neumann boundary conditions at $\{x = 0\}$. Also, we need to introduce noise in the data and to consider an exact, noiseless solution. By one of the concepts of the regularization theory, we assume that there exists an exact solution $a^*(x) \in C^1(\mathbb{R})$ of the CIP (1.3)-(1.4) with the noiseless data [6, 36], and this function satisfies conditions (1.1), (1.2). Let w^* be the function w which corresponds to $a^*(x)$. We assume that $w^* \in B(d, p_0^*, p_1^*)$, where p_0^*, p_1^* are the noiseless data p_0, p_1 . Let $\xi \in (0, 1)$ be the level of noise in the data. Obviously there exists a function $G^* \in B(d, p_0^*, p_1^*)$. Suppose that there exists a function $G \in B(d, p_0, p_1)$ such that

$$\|G - G^*\|_{H^3(R)} < \xi. \quad (4.5)$$

Denote $W^* = w^* - G^*$ and $W = w - G$, $\forall w \in B(d, p_0, p_1)$,

$$B_0(D) = \left\{ U \in H_0^3(R) : \|U\|_{H^3(R)} < D \right\}, \quad \forall D > 0.$$

Then (3.4) and the triangle inequality imply that

$$W^* \in B_0(2d), \quad W \in B_0(2d), \quad \forall w \in B(d, p_0, p_1), \quad (4.6)$$

$$W + G \in B(3d, p_0, p_1), \quad \forall W \in B_0(2d). \quad (4.7)$$

Denote

$$I_{\lambda, \beta}(W) = J_{\lambda, \beta}(W + G), \quad \forall W \in B_0(2d).$$

Theorem 4.4. The Fréchet derivative $I'_{\lambda, \beta}(W) \in H_0^3(R)$ of the functional $I_{\lambda, \beta}(W)$ exists for every point $W \in \overline{B_0(2d)}$ and for all $\lambda, \beta > 0$. Let $\lambda_1 = \lambda_1(\alpha, \varepsilon, d)$ be the number of Theorem 4.2. Denote $\lambda_2 = \lambda_1(\alpha, \varepsilon, 3d) \geq \lambda_1$. Let $\lambda \geq \lambda_2$ and also let $\beta \in [2e^{-\lambda\alpha T}, 1)$.

Then the functional $I_{\lambda,\beta}(W)$ is strictly convex on the ball $\overline{B_0(2d)} \subset H_0^3(R)$. More precisely, the following estimate holds:

$$\begin{aligned} I_{\lambda,\beta}(W_2) - I_{\lambda,\beta}(W_1) - I'_{\lambda,\beta}(W_1)(W_2 - W_1) &\geq C_1 e^{-2\lambda(2\alpha-\varepsilon)} \|W_2 - W_1\|_{H^1(Tr_{\alpha,\varepsilon})}^2 \\ &+ C_1 e^{-2\lambda(2\alpha-\varepsilon)} \|W_2(x,0) - W_1(x,0)\|_{H^1(0,2\alpha-\varepsilon)}^2 + \frac{\beta}{2} \|W_2 - W_1\|_{H^3(R)}^2, \quad (4.8) \\ &\forall w_1, w_2 \in \overline{B_0(2d)}, \forall \lambda \geq \lambda_2. \end{aligned}$$

Furthermore, there exists a unique minimized $W_{\min,\lambda,\beta} \in \overline{B_0(2d)}$ of the functional $I_{\lambda,\beta}(W)$ and the following inequality holds

$$I'_{\lambda,\beta}(W_{\min,\lambda,\beta})(W - W_{\min,\lambda,\beta}) \geq 0, \quad \forall W \in \overline{B_0(2d)}. \quad (4.9)$$

Theorem 4.5. (*the accuracy of the minimizer*). Let the number $T \geq 4$. Denote

$$\sigma = \frac{\alpha(T-4) + \varepsilon}{2(2\alpha-\varepsilon)}, \quad \rho = \frac{1}{2} \min(\sigma, 1) \in \left(0, \frac{1}{2}\right). \quad (4.10)$$

Choose a number $\xi_0 \in (0, 1)$ so small that $\ln \xi_0^{-1/(2(2\alpha-\varepsilon))} \geq \lambda_2$, where λ_2 is the number of Theorem 4.4. Let the level of noise in the data $\xi \in (0, \xi_0)$. Choose the parameters $\lambda = \lambda(\xi)$ and $\beta = \beta(\xi)$ as

$$\lambda = \lambda(\xi) = \ln \xi^{-1/(2(2\alpha-\varepsilon))} > \lambda_2, \quad \beta = \beta(\xi) = 2e^{-\lambda\alpha T} = 2\xi^{(\alpha T)/(2(2\alpha-\varepsilon))} \quad (4.11)$$

(see Theorem 4.2 for β). Then the following accuracy estimates are valid:

$$\|w_{\min,\lambda,\beta} - w^*\|_{H^1(Tr_{\alpha,\varepsilon})} \leq C_1 \xi^\rho, \quad \|a_{\min,\lambda,\beta} - a^*\|_{L^2(0,2\alpha-\varepsilon)} \leq C_1 \xi^\rho, \quad (4.12)$$

where $w_{\min,\lambda,\beta} = (W_{\min,\lambda,\beta} + G) \in \overline{B(3d, p_0, p_1)}$. Here, $W_{\min,\lambda,\beta} \in \overline{B_0(2d)}$ is the minimizer, which is found in Theorem 4.4, and $a_{\min,\lambda,\beta}(x) = 2\partial_x[w_{\min,\lambda,\beta}(x,0)]$, as in (2.27).

We now construct the gradient projection method of the minimization of the functional $I_{\lambda,\beta}(W)$ on the closed ball $B_0(2d) \subset H_0^3(R)$. Let $P_{B_0} : H_0^3(R) \rightarrow B_0(2d)$ be the orthogonal projection operator. Let $W_0 \in B_0(2d)$ be an arbitrary point and the number $\gamma \in (0, 1)$. The sequence of the gradient projection method is [2]:

$$W_n = P_{B_0}(W_{n-1} - \gamma I'_{\lambda,\beta}(W_{n-1})), \quad n = 1, 2, \dots \quad (4.13)$$

Theorem 4.6. (*the global convergence of the gradient projection method*).

Let $\lambda_2 = \lambda_1(\alpha, \varepsilon, 3d) \geq \lambda_1$, where $\lambda_1 \geq 1$ is the number of Theorem 4.2. Let the numbers $T, \rho, \xi_0, \xi \in (0, \xi_0), \lambda(\xi)$ and $\beta(\xi)$ be the same as in Theorem 4.5. Let $W_{\min,\lambda,\beta} \in \overline{B_0(2d)}$ be the unique minimizer of the functional $I_{\lambda,\beta}(W)$, as in Theorem 4.4. Also, as in Theorem 4.4, denote $w_{\min,\lambda,\beta} = (W_{\min,\lambda,\beta} + G) \in \overline{B(3d, p_0, p_1)}$ and let $w_n = (W_n + G) \in \overline{B(3d, p_0, p_1)}$, where $n = 0, 1, \dots$. Also, let $a_{\min,\lambda,\beta}(x)$ and $a_n(x)$ be the approximations of the coefficient $a^*(x)$, which are found from the functions $w_{\min,\lambda,\beta}$ and w_n respectively via (2.27). Then there exists a number $\gamma_0 = \gamma_0(\alpha, \varepsilon, d, \xi) \in (0, 1)$ depending only on listed parameters such that for any $\gamma \in (0, \gamma_0)$ there exists a number $\theta = \theta(\gamma) \in (0, 1)$ such that the following convergence rates hold:

$$\|w_{\min,\lambda,\beta} - w_n\|_{H^3(R)} \leq \theta^n \|w_{\min,\lambda,\beta} - w_0\|_{H^3(R)}, \quad n = 1, 2, \dots, \quad (4.14)$$

$$\|a_{\min,\lambda,\beta} - a_n\|_{H^1(0,2\alpha-\varepsilon)} \leq \theta^n \|w_{\min,\lambda,\beta} - w_0\|_{H^3(R)}, \quad n = 1, 2, \dots, \quad (4.15)$$

$$\|w^* - w_n\|_{H^1(Tr_{\alpha,\varepsilon})} \leq C_1 \xi^\rho + \theta^n \|w_{\min,\lambda,\beta} - w_0\|_{H^3(R)}, \quad n = 1, 2, \dots, \quad (4.16)$$

$$\|a^* - a_n\|_{L^2(Tr_{\alpha,\varepsilon})} \leq C_1 \xi^\rho + \theta^n \|w_{\min,\lambda,\beta} - w_0\|_{H^3(R)}, \quad n = 1, 2, \dots \quad (4.17)$$

Remark 5. 1. Since the starting point W_0 of iterations of the gradient projection method (4.13) is an arbitrary point of the ball $B_0(2d)$ and since the radius $d > 0$ of this ball is an arbitrary number, then estimates (4.14)-(4.17) ensure the global convergence of the sequence (4.13) to the correct solution, see the first sentence of Introduction.

2. We omit below the proofs of Theorem 4.3 and 4.4. Indeed, Theorem 4.3 follows immediately from the combination of Theorem 4.2 with Lemma 2.1 of [2]. Also, Theorem 4.4 follows immediately from Theorems 4.2, 4.3, (4.6) and (4.7).

5. Proofs. Below in this section $(x, t) \in R$, where R is the rectangle defined in (3.2).

5.1. Proof of Theorem 4.1. In this proof $C = C(\alpha) > 0$ denotes different constants depending only on α . We assume in this proof that the function $u \in C^2(\bar{R}) \cap H_0^2(R)$. The more general case $u \in H_0^2(R)$ can be obtained from this one via density arguments. Introduce a new function

$$v(x, t) = u(x, t) e^{-\lambda(x+\alpha t)} \quad (5.1)$$

and express $u_{xx} - 2u_{xt}$ via derivatives of the function $v(x, t)$. We obtain:

$$\begin{aligned} u &= v e^{\lambda(x+\alpha t)}, \quad u_x = (v_x + \lambda v) e^{\lambda(x+\alpha t)}, \quad u_t = (v_t + \lambda \alpha v) e^{\lambda(x+\alpha t)}, \\ u_{xx} &= (v_{xx} + 2\lambda v_x + \lambda^2 v) e^{\lambda(x+\alpha t)}, \quad u_{xt} = (v_{xt} + \lambda \alpha v_x + \lambda v_t + \lambda^2 \alpha v) e^{\lambda(x+\alpha t)}, \\ (u_{xx} - 2u_{xt})^2 e^{-2\lambda(x+\alpha t)} &= [(v_{xx} - 2v_{xt} + \lambda^2(1 - 2\alpha)v) + (2\lambda(1 - \alpha)v_x - 2\lambda v_t)]^2. \end{aligned}$$

Hence,

$$\begin{aligned} (u_{xx} - 2u_{xt})^2 e^{-2\lambda(x+\alpha t)} &\geq \frac{(u_{xx} - 2u_{xt})^2 e^{-2\lambda(x+\alpha t)}}{x+1} \geq \\ &\frac{(4\lambda(1 - \alpha)v_x - 4\lambda v_t)(v_{xx} - 2v_{xt} + \lambda^2(1 - 2\alpha)v)}{x+1}. \end{aligned} \quad (5.2)$$

We estimate from below in two steps two products in the second line of (5.2) involving v_x and v_t .

Step 1. Estimate

$$\begin{aligned} \frac{4\lambda(1 - \alpha)v_x(v_{xx} - 2v_{xt} + \lambda^2(1 - 2\alpha)v)}{x+1} &= \left(\frac{2\lambda(1 - \alpha)v_x^2}{x+1} \right)_x + \frac{2\lambda(1 - \alpha)v_x^2}{(x+1)^2} + \\ &\left(-\frac{4\lambda(1 - \alpha)v_x^2}{x+1} \right)_t + \left(\frac{2\lambda^3(1 - \alpha)(1 - 2\alpha)v^2}{x+1} \right)_x + \frac{2\lambda^3(1 - \alpha)(1 - 2\alpha)v^2}{(x+1)^2}. \end{aligned}$$

Thus, we have obtained on the first step:

$$\begin{aligned} \frac{4\lambda(1 - \alpha)v_x(v_{xx} - 2v_{xt} + \lambda^2(1 - 2\alpha)v)}{x+1} &= \frac{2\lambda(1 - \alpha)v_x^2}{(x+1)^2} + \frac{2\lambda^3(1 - \alpha)(1 - 2\alpha)v^2}{(x+1)^2} + \\ &\left(\frac{2\lambda(1 - \alpha)v_x^2}{x+1} + \frac{2\lambda^3(1 - \alpha)(1 - 2\alpha)v^2}{x+1} \right)_x + \left(-\frac{4\lambda(1 - \alpha)v_x^2}{x+1} \right)_t. \end{aligned} \quad (5.3)$$

Step 2. Estimate

$$\begin{aligned}
& -\frac{4\lambda v_t (v_{xx} - 2v_{xt} + \lambda^2(1-2\alpha)v)}{x+1} = \left(-\frac{4\lambda v_t v_x}{x+1}\right)_x + \frac{4\lambda v_{xt} v_x}{x+1} - \frac{4\lambda v_t v_x}{(x+1)^2} + \\
& \left(\frac{4\lambda v_t^2}{x+1}\right)_x + \frac{4\lambda v_t^2}{(x+1)^2} + \left(-\frac{2\lambda^3(1-2\alpha)v^2}{x+1}\right)_t = \frac{4\lambda v_t^2 - 4\lambda v_t v_x}{(x+1)^2} + \\
& \left(\frac{2\lambda v_x^2 - 2\lambda^3(1-2\alpha)v^2}{x+1}\right)_t + \left(\frac{4\lambda v_t^2 - 4\lambda v_t v_x}{x+1}\right)_x.
\end{aligned}$$

Thus,

$$\begin{aligned}
& -\frac{4\lambda v_t (v_{xx} - 2v_{xt} + \lambda^2(1-2\alpha)v)}{x+1} = \frac{4\lambda v_t^2}{(x+1)^2} - \frac{4\lambda v_t v_x}{(x+1)^2} \\
& \left(\frac{2\lambda v_x^2 - 2\lambda^3(1-2\alpha)v^2}{x+1}\right)_t + \left(\frac{4\lambda v_t^2 - 4\lambda v_t v_x}{x+1}\right)_x. \tag{5.4}
\end{aligned}$$

Summing up (5.3) with (5.4) and taking into account (5.2), we obtain

$$\begin{aligned}
& (u_{xx} - 2u_{xt})^2 e^{-2\lambda(x+\alpha t)} \geq \frac{2\lambda}{(x+1)^2} [(1-\alpha)v_x^2 - 2v_x v_t + 2v_t^2] + \\
& \frac{2\lambda^3(1-\alpha)(1-2\alpha)v^2}{(x+1)^2} + \left(\frac{-2(1-2\alpha)(\lambda v_x^2 + \lambda^3 v^2)}{x+1}\right)_t \\
& + \left(\frac{2\lambda(1-\alpha)v_x^2 - 4\lambda v_t v_x + 4\lambda v_t^2}{x+1} + \frac{2\lambda^3(1-\alpha)(1-2\alpha)v^2}{x+1}\right)_x. \tag{5.5}
\end{aligned}$$

Hence, by Young's inequality

$$2\lambda(1-\alpha)v_x^2 - 4\lambda v_t v_x + 4\lambda v_t^2 \geq 2\lambda \left[(1-\alpha-\varepsilon)v_x^2 + \left(2-\frac{1}{\varepsilon}\right)v_t^2 \right]. \tag{5.6}$$

Thus, in order to ensure the positivity of both terms in the right hand side of (5.6), we should have $1/2 < \varepsilon < 1-\alpha$. We take ε as the average of lower and upper bounds of these two inequalities,

$$\varepsilon = \frac{1}{2} \left(\frac{1}{2} + (1-\alpha) \right) = \frac{3-2\alpha}{4}.$$

Hence, (5.6) becomes

$$2\lambda(1-\alpha)v_x^2 - 4\lambda v_t v_x + 4\lambda v_t^2 \geq \frac{\lambda(1-2\alpha)}{2} v_x^2 + \frac{4\lambda(1-2\alpha)}{3-2\alpha} v_t^2. \tag{5.7}$$

Note that since $u \in C^2(\bar{R}) \cap H_0^2(R)$, then by (5.1) $v(0, t) = v_x(0, t) = 0$. Hence, integrating (5.5) over R and taking into account (5.7), we obtain

$$\begin{aligned}
& \int_R (u_{xx} - 2u_{xt})^2 e^{-2\lambda(x+\alpha t)} \geq C\lambda \int_R (v_x^2 + v_t^2) dxdt + C\lambda^3 \int_R v^2 dxdt \\
& + C\lambda \int_0^1 v_x^2(x, 0) dx + C\lambda^3 \int_0^1 v^2(x, 0) dx - C\lambda \int_0^1 v_x^2(x, T) dx - C\lambda^3 \int_0^1 v^2(x, T) dx. \tag{5.8}
\end{aligned}$$

We now replace in (5.8) the function v with the function u via (5.1). We have

$$\begin{aligned}\lambda v_x^2 &= \lambda (u_x^2 - 2\lambda u_x u + \lambda^2 u^2) e^{-2\lambda(x+\alpha t)} \geq \left(\frac{\lambda}{2} u_x^2 - \lambda^3 u^2\right) e^{-2\lambda(x+\alpha t)}, \\ \lambda v_t^2 &= \lambda (u_t^2 - 2\lambda \alpha u_t u + \lambda^2 \alpha^2 u^2) e^{-2\lambda(x+\alpha t)} \geq \left(\frac{\lambda}{2} u_t^2 - \lambda^3 \alpha^2 u^2\right) e^{-2\lambda(x+\alpha t)}.\end{aligned}$$

Thus,

$$C\lambda (v_x^2 + v_t^2) \geq \frac{C}{4}\lambda (v_x^2 + v_t^2) \geq \left(\frac{C}{8}\lambda (u_x^2 + u_t^2) - \frac{C}{2}\lambda^3 u^2\right) e^{-2\lambda(x+\alpha t)}.$$

Hence, (5.8) implies the following estimate, which is equivalent with (4.1):

$$\begin{aligned}\int_R (u_{xx} - 2u_{xt})^2 e^{-2\lambda(x+\alpha t)} &\geq \frac{C}{8}\lambda \int_R (u_x^2 + u_t^2) e^{-2\lambda(x+\alpha t)} dx dt \\ &+ \frac{C}{2}\lambda^3 \int_R u^2 e^{-2\lambda(x+\alpha t)} dx dt + \frac{C}{8}\lambda \int_0^1 u_x^2(x, 0) e^{-2\lambda x} dx \\ &+ \frac{C}{2}\lambda^3 \int_0^1 u^2(x, 0) e^{-2\lambda x} dx - C\lambda e^{-2\lambda\alpha T} \int_0^1 u_x^2(x, T) dx - C\lambda^3 e^{-2\lambda\alpha T} \int_0^1 u^2(x, T) dx. \quad \square\end{aligned}$$

5.2. Proof of Theorem 4.2. Let two arbitrary functions $w_1, w_2 \in \overline{B(d, p_0, p_1)}$. Denote $h = w_2 - w_1$. Then $h \in \overline{B_0(2d)}$. Note that embedding theorem implies that sets $\overline{B(d, p_0, p_1)}, \overline{B_0(2d)} \subset C^1(\overline{R})$,

$$\|w\|_{C^1(\overline{R})} \leq C_1, \quad \forall w \in \overline{B(d, p_0, p_1)}, \quad \|h\|_{C^1(\overline{R})} \leq C_1. \quad (5.9)$$

It follows from (3.5) that in this proof, we should first estimate from below $[L(w_1 + h)]^2 - [L(w_1)]^2$. We will single out the linear and nonlinear parts, with respect to h , of this expression. By (2.18):

$$\begin{aligned}L(w_1 + h) &= L(w_1) + h_{xx} - 2h_{xt} + 2h_x \int_0^t w_{1x}(x, \tau) d\tau + 2w_{1x} \int_0^t h_x(x, \tau) d\tau \\ &- 2h_x w_1 - 2h_x h - 2w_{1x} h - 2h_t \int_0^t w_{1x}(x, \tau) d\tau - 2w_{1t} \int_0^t h_x(x, \tau) d\tau \\ &+ 2 \left[h_x \int_0^t h_x(x, \tau) d\tau - h_t \int_0^t h_x(x, \tau) d\tau \right] = L(w_1) + L_{lin}(h) + L_{nl}(h),\end{aligned} \quad (5.10)$$

where $L_{lin}(h)$ and $L_{nl}(h)$ are linear and nonlinear, with respect to h , parts of (5.10), and their forms are clear from (5.10). Hence,

$$\begin{aligned}[L(w_1 + h)]^2 - [L(w_1)]^2 &= 2L(w_1)L_{lin}(h) + (L_{lin}(h))^2 + \\ &(L_{nl}(h))^2 + 2L_{lin}(h)L_{nl}(h) + 2L(w_1)L_{nl}(h).\end{aligned} \quad (5.11)$$

Using (5.9), (5.10) and the Cauchy-Schwarz inequality, we obtain

$$\begin{aligned} & (L_{lin}(h))^2 + (L_{nl}(h))^2 + 2L_{lin}(h)L_{nl}(h) + 2L(w_1)L_{nl}(h) \\ & \geq \frac{1}{2}(h_{xx} - 2h_{xt})^2 - C_1 \left[h_x^2 + h_t^2 + h^2 + \left(\int_0^t h_x(x, \tau) d\tau \right)^2 \right]. \end{aligned} \quad (5.12)$$

Let (\cdot, \cdot) denotes the scalar product in $H^3(R)$. It follows from (3.5) and (5.11) that

$$J_{\lambda, \beta}(w_1 + h) - J_{\lambda, \beta}(w_1) = A(h) + B(h), \quad (5.13)$$

where $A(h) : H_0^3(R) \rightarrow \mathbb{R}$ is a bounded linear functional,

$$A(h) = \int_R 2L(w_1)L_{lin}(h)\varphi_\lambda dxdt + 2\beta(w_1, h)$$

and $B(h)$ is a nonlinear functional,

$$B(h) = \quad (5.14)$$

$$\int_R \left[(L_{lin}(h))^2 + (L_{nl}(h))^2 + 2L_{lin}(h)L_{nl}(h) + 2L(w_1)L_{nl}(h) \right] \varphi_\lambda dxdt + \beta \|h\|_{H^3(R)}^2.$$

By the Riesz theorem, there exists unique point $\tilde{A} \in H_0^3(R)$ such that

$$A(h) = (\tilde{A}, h), \quad \forall h \in H_0^3(R). \quad (5.15)$$

Next, it follows from (5.13)-(5.15) that

$$\lim_{\|h\|_{H^3(R)} \rightarrow 0} \frac{|J_{\lambda, \beta}(w_1 + h) - J_{\lambda, \beta}(w_1) - (\tilde{A}, h)|}{\|h\|_{H^3(R)}} = 0.$$

Hence, $\tilde{A} \in H_0^3(R)$ is the Fréchet derivative $J'_{\lambda, \beta}(w_1) \in H_0^3(R)$ of the functional $J_{\lambda, \beta}(w_1)$ at the point w_1 ,

$$\tilde{A} = J'_{\lambda, \beta}(w_1). \quad (5.16)$$

Next, (3.5) and (5.12)-(5.16) imply that for all $\lambda \geq 1$

$$\begin{aligned} & J_{\lambda, \beta}(w_1 + h) - J_{\lambda, \beta}(w_1) - J'_{\lambda, \beta}(w_1)(h) \geq \frac{1}{2} \int_R (h_{xx} - 2h_{xt})^2 \varphi_\lambda dxdt \\ & - C_1 \int_R \left[h_x^2 + h_t^2 + h^2 + \left(\int_0^t h_x(x, \tau) d\tau \right)^2 \right] \varphi_\lambda dxdt + \beta \|h\|_{H^3(R)}^2. \end{aligned} \quad (5.17)$$

Combining Lemma 3.1, Theorem 4.1 and (5.17) and also assuming that $\lambda \geq \lambda_0$, we obtain

$$\begin{aligned}
& J_{\lambda,\beta}(w_1+h) - J_{\lambda,\beta}(w_1) - J'_{\lambda,\beta}(w_1)(h) \geq C\lambda \int_R (h_x^2 + h_t^2) \varphi_\lambda dxdt \\
& + C\lambda^3 \int_R h^2 \varphi_\lambda dxdt + \beta \|h\|_{H^3(R)}^2 - C_1 \int_R (h_x^2 + h_t^2 + h^2) \varphi_\lambda dxdt \\
& + C\lambda \int_0^1 h_x^2(x,0) e^{-2\lambda x} dx + C\lambda^3 \int_0^1 h^2(x,0) e^{-2\lambda x} dx \\
& - C\lambda e^{-2\lambda\alpha T} \int_0^1 h_x^2(x,T) dx - C\lambda^3 e^{-2\lambda\alpha T} \int_0^1 h^2(x,T) dx.
\end{aligned} \tag{5.18}$$

Choose $\lambda_1 = \lambda_1(\alpha, \varepsilon, d) \geq \lambda_0 \geq 1$ so large that $C\lambda_1 > 2C_1$ and then take in (5.18) $\lambda \geq \lambda_1$. We obtain

$$\begin{aligned}
& J_{\lambda,\beta}(w_1+h) - J_{\lambda,\beta}(w_1) - J'_{\lambda,\beta}(w_1)(h) \geq C_1\lambda \int_R (h_x^2 + h_t^2) \varphi_\lambda dxdt \\
& + C_1\lambda^3 \int_R h^2 \varphi_\lambda dxdt + C_1\lambda \int_0^1 h_x^2(x,0) e^{-2\lambda x} dx + C_1\lambda^3 \int_0^1 h^2(x,0) e^{-2\lambda x} dx \\
& + \beta \|h\|_{H^3(R)}^2 - C_1\lambda e^{-2\lambda\alpha T} \int_0^1 h_x^2(x,T) dx - C_1\lambda^3 e^{-2\lambda\alpha T} \int_0^1 h^2(x,T) dx.
\end{aligned} \tag{5.19}$$

Since $Tr_{\alpha,\varepsilon} \subset Tr \subset R$ and since the interval $(0, 2\alpha - \varepsilon) \subset (0, 1)$ and also since $\varphi_\lambda(x, t) \geq e^{-2\lambda(2\alpha - \varepsilon)}$ in $Tr_{\alpha,\varepsilon}$, then we obtain from (5.19)

$$\begin{aligned}
& J_{\lambda,\beta}(w_1+h) - J_{\lambda,\beta}(w_1) - J'_{\lambda,\beta}(w_1)(h) \geq C_1 e^{-2\lambda(2\alpha - \varepsilon)} \|h\|_{H^1(Tr_{\alpha,\varepsilon})}^2 + \\
& C_1 e^{-2\lambda(2\alpha - \varepsilon)} \|h(x,0)\|_{H^1(0,2\alpha - \varepsilon)}^2 + \beta \|h\|_{H^3(R)}^2 - C_1\lambda^3 e^{-2\lambda\alpha T} \|h(x,T)\|_{H^1(Tr_{\alpha,\varepsilon})}^2, \quad \forall \lambda \geq \lambda_1.
\end{aligned}$$

By the trace theorem $\|h(x,T)\|_{H^1(0,2\alpha - \varepsilon)}^2 \leq C_1 \|h\|_{H^3(R)}^2$. Hence, taking $\beta \in [2e^{-\lambda\alpha T}, 1)$, we obtain the following estimate for all $\lambda \geq \lambda_1$:

$$\begin{aligned}
& J_{\lambda,\beta}(w_1+h) - J_{\lambda,\beta}(w_1) - J'_{\lambda,\beta}(w_1)(h) \geq C_1 e^{-2\lambda(2\alpha - \varepsilon)} \|h\|_{H^1(Tr_{\alpha,\varepsilon})}^2 \\
& + C_1 e^{-2\lambda(2\alpha - \varepsilon)} \|h(x,0)\|_{H^1(0,2\alpha - \varepsilon)}^2 + \frac{\beta}{2} \|h\|_{H^3(R)}^2.
\end{aligned} \tag{5.20}$$

This estimate is equivalent with our target estimate (4.3). \square

5.3. Proof of Theorem 4.5. Let $\lambda \geq \lambda_2$. Temporary denote $I_{\lambda,\beta}(W, G) := J_{\lambda,\beta}(W + G)$. Consider $I_{\lambda,\beta}(W^*, G)$,

$$\begin{aligned}
I_{\lambda,\beta}(W^*, G) &= J_{\lambda,\beta}(W^* + G) = \int_R [L(W^* + G)]^2 \varphi_\lambda dxdt + \beta \|W^* + G\|_{H^3(R)}^2 = \\
& J_{\lambda,\beta}^0(W^* + G) + \beta \|W^* + G\|_{H^3(R)}^2
\end{aligned} \tag{5.21}$$

Since $L(W^* + G^*) = L(w^*) = 0$, then

$$L(W^* + G) = L(W^* + G^* + (G - G^*)) = L(W^* + G^*) + \widehat{L}(G - G^*) = \widehat{L}(G - G^*),$$

where by (2.18) and (4.5), $\left| \widehat{L}(G - G^*)(x, t) \right| \leq C_1 \xi$ for all $(x, t) \in \bar{R}$. Hence, by (5.21)

$$I_{\lambda, \beta}(W^*, G) \leq C_1 (\xi^2 + \beta). \quad (5.22)$$

We have

$$W^* - W_{\min, \lambda, \beta} = (W^* + G) - (W_{\min, \lambda, \beta} + G) = (w^* - w_{\min, \lambda, \beta}) + (G - G^*). \quad (5.23)$$

Also, by (4.5) and the trace theorem

$$\|G(x, 0) - G^*(x, 0)\|_{H^1(0, 2\alpha - \varepsilon)} \leq C_1 \xi. \quad (5.24)$$

Hence, (4.5), (5.23) and (5.24) imply

$$\begin{aligned} \|W^* - W_{\min, \lambda, \beta}\|_{H^1(Tr_{\alpha, \varepsilon})}^2 &\geq \frac{1}{2} \|w^* - w_{\min, \lambda, \beta}\|_{H^1(Tr_{\alpha, \varepsilon})}^2 - C_1 \xi^2, \\ \|W^*(x, 0) - W_{\min, \lambda, \beta}(x, 0)\|_{H^1(0, 2\alpha - \varepsilon)}^2 &\geq \frac{1}{2} \|w^* - w_{\min, \lambda, \beta}\|_{H^1(0, 2\alpha - \varepsilon)}^2 - C_1 \xi^2 \\ \frac{\beta}{2} \|W^* - W_{\min, \lambda, \beta}\|_{H^3(R)}^2 &\geq \frac{\beta}{4} \|w^* - w_{\min, \lambda, \beta}\|_{H^3(R)}^2 - \frac{\beta}{2} \xi^2 \end{aligned}$$

Hence, using (4.8), we obtain

$$\begin{aligned} I_{\lambda, \beta}(W^*, G) - I_{\lambda, \beta}(W_{\min, \lambda, \beta}, G) - I'_{\lambda, \beta}(W_{\min, \lambda, \beta}, G)(W^* - W_{\min, \lambda, \beta}) &\geq \\ C_1 e^{-2\lambda(2\alpha - \varepsilon)} \|w^* - w_{\min, \lambda, \beta}\|_{H^1(Tr_{\alpha, \varepsilon})}^2 - C_1 \xi^2 & \quad (5.25) \\ + C_1 e^{-2\lambda(2\alpha - \varepsilon)} \|w^*(x, 0) - w_{\min, \lambda, \beta}(x, 0)\|_{H^1(0, 2\alpha - \varepsilon)}^2 & \end{aligned}$$

By (4.9)

$$-I'_{\lambda, \beta}(W_{\min, \lambda, \beta}, G)(W^* - W_{\min, \lambda, \beta}) \leq 0.$$

Hence,

$$I_{\lambda, \beta}(W^*, G) - I_{\lambda, \beta}(W_{\min, \lambda, \beta}, G) - I'_{\lambda, \beta}(W_{\min, \lambda, \beta}, G)(W^* - W_{\min, \lambda, \beta}) \leq I_{\lambda, \beta}(W^*, G).$$

Comparing this with (5.22) with (5.25) and dropping the term with β in (5.25), we obtain

$$\begin{aligned} e^{-2\lambda(2\alpha - \varepsilon)} \left(\|w^* - w_{\min, \lambda, \beta}\|_{H^1(Tr_{\alpha, \varepsilon})}^2 + \|w^*(x, 0) - w_{\min, \lambda, \beta}(x, 0)\|_{H^1(0, 2\alpha - \varepsilon)}^2 \right) & \quad (5.26) \\ \leq C_1 (\xi^2 + \beta). & \end{aligned}$$

Dividing both sides of (5.26) by $e^{-2\lambda(2\alpha - \varepsilon)}$ and recalling that by (4.11) $\beta = 2e^{-\lambda\alpha T}$, we obtain

$$\begin{aligned} \|w^* - w_{\min, \lambda, \beta}\|_{H^1(Tr_{\alpha, \varepsilon})}^2 + \|w^*(x, 0) - w_{\min, \lambda, \beta}(x, 0)\|_{H^1(0, 2\alpha - \varepsilon)}^2 & \\ \leq C_1 \xi^2 e^{2\lambda(2\alpha - \varepsilon)} + C_1 \exp(-\lambda(\alpha(T - 4) + 2\varepsilon)). & \quad (5.27) \end{aligned}$$

Since $T \geq 4$, then $-\lambda(\alpha(T - 4) + 2\varepsilon) < 0$. Since we have chosen $\lambda = \lambda(\xi)$ and $\beta = \beta(\xi)$ as in (4.11), then in (5.27) $\xi^2 e^{2\lambda(2\alpha - \varepsilon)} = \xi$ and $\exp(-\lambda(\alpha(T - 4) + 2\varepsilon)) = \xi^\sigma$. Hence, target estimates (4.12) follow from (2.27), (4.10) and (5.27). \square

5.4. Proof of Theorem 4.6. The existence of the number $\theta \in (0, 1)$ as well as convergence rates (4.14) and (4.15) follow immediately from a combination of Theorem 4.2 with Theorem 2.1 of [2]. Convergence rate (4.16) follows immediately from the triangle inequality, (4.12) and (4.14). Similarly, convergence rate (4.17) follows immediately from the triangle inequality, (4.12) and (4.15). \square

6. Numerical Implementation. To computationally simulate the data (1.4) for our CIP, we solve the forward problem (2.24)-(2.26) by the finite difference method in the domain $\{(x, t) \in (-A, A) \times (0, T)\}$. In all our computations of the forward problem (2.24)-(2.26) we take $A = B = 2.2, T = 4$. For a given function $a(x)$ we compute the solution $u_{i,j} = u(x_i, t_j)$ on the rectangular mesh with $N_x = 1024$ spatial and $N_t = 1024$ temporal grid points.

Now, even though Theorems 4.5 and 4.6 work only for $T \geq 4$, we use $T = 2$ in our computations of the inverse problem. Also, when computing the inverse problem, we take $A = 1.1$. Thus, the rectangle R in (3.2) is replaced in our computations of the inverse problem with the rectangle R' ,

$$R' = (0, A) \times (0, T) = (0, 1.1) \times (0, 2).$$

In order to avoid the inverse crime, we work in the inverse problem with the rectangular mesh of $N_x \times N_t = 60 \times 50$ grid points. The absorbing boundary condition (2.26) at $x = A$ gives us the following direct analog of boundary condition (3.3):

$$w_x(1.1, t) = 0. \quad (6.1)$$

We have observed numerically that this condition provides a better stability for our computations of the inverse problem, as compared with the case when condition (6.1) is absent.

The finite difference approximations of differential operators in (2.18) are used on the rectangular mesh with $h = (h_x, h_t)$. Denote $w(x_i, t_j) = w^{i,j}$. We write the functional $J_{\lambda, \beta}(w)$ in (3.5) in the finite difference form as:

$$\begin{aligned} J_{\lambda, \beta, \mu}^h(w^{i,j}) &= h_x h_t \sum_{i=3}^{N_x-1} \sum_{j=1}^{N_t-1} \left(\frac{w^{i,j} - 2w^{i+1,j} + w^{i+2,j}}{h_x^2} \right. \\ &\quad - 2 \frac{w^{i+1,j+1} - w^{i+1,j} - w^{i,j+1} + w^{i,j}}{h_x h_t} \\ &\quad + 2h_t \frac{w^{i+1,j} - w^{i,j}}{h_x} \sum_{l=1}^{N_t-1} \left(\frac{w^{i+1,l} - w^{i,l}}{h_x} \right) - 2 \frac{w^{i+1,j} - w^{i,j}}{h_x} w^{i,j} \\ &\quad \left. - 2(w^{i,j+1} - w^{i,j}) \sum_{l=1}^{N_t-1} \left(\frac{w^{i+1,l} - w^{i,l}}{h_x} \right)^2 e^{-2\lambda(x_i + \alpha t_j)} \right) \\ &\quad + \beta h_x h_t \sum_{i=3}^{N_x-1} \sum_{j=1}^{N_t-1} \left((w^{i,j})^2 + \left(\frac{w^{i+1,j} - w^{i,j}}{h_x} \right)^2 + \left(\frac{w^{i,j+1} - w^{i,j}}{h_t} \right)^2 \right. \\ &\quad \left. + \left(\frac{w^{i,j} - 2w^{i+1,j} + w^{i+2,j}}{h_x^2} \right)^2 + \left(\frac{w^{i,j} - 2w^{i,j+1} + w^{i,j+2}}{h_t^2} \right)^2 \right) \\ &\quad + \mu \sum_{j=1}^{N_t-1} \left(\frac{w^{N_x,j} - w^{N_x-1,j}}{h_x} \right)^2. \end{aligned} \quad (6.2)$$

Next, we minimize functional (6.2) with respect to the values $w^{i,j}$ of the unknown function $w(x, t)$ at grid points (x_i, t_j) . To speed up computations, the gradient of the functional (6.2) is written in an explicit form, using Kronecker symbols, as in [25]. For brevity, we do not bring in these formulas here.

Remark 6. 1. In fact the functional (6.2), which is used to conduct numerical studies, is a slightly modified finite difference version of (3.5). In our computations, we took the Tikhonov regularization term in the finite difference analog of $H^2(R')$ instead of $H^3(R')$. Note that since the number of grid points is not exceedingly large here ($N_x = 60, N_t = 50$),

then all discrete norms are basically equivalent. Additionally, the boundary term with the coefficient $\mu \gg 1$ is added in (6.2) to ensure that the minimizer satisfies boundary condition (6.1).

2. We choose parameters λ, α, β and μ so that the numerical method provides a good reconstruction of a reference function $a(x)$ of our choice depicted on Figure 3(A). The values of our parameters were found by the trial and error procedure. It is important though that exactly the same values of those parameters were used then in three subsequent tests. Those values were:

$$\lambda = 2, \alpha = 1/2, \beta = 10^{-4}, \mu = 10^2. \quad (6.3)$$

We note that even though the parameter λ has to be sufficiently large, $\lambda = 2$ worked quite well in our numerical experiments. This is similar with all above cited works about numerical studies of the convexification. The topic of optimal choices of these parameters is outside of the scope of this paper. Also, see below a brief discussion of the choice of parameters λ and α .

3. Even though Theorem 4.6 guarantees the global convergence of the gradient projection method, we have observed in our computations that just the straightforward gradient descent method works well. This method is simpler to implement than the gradient projection method since one does not need to use the orthogonal projection operator P_{B_0} in (4.13). Thus, we have not subtracted the function G from the function w and minimized, therefore, the functional $J_{\lambda, \beta}$ instead of the functional $I_{\lambda, \beta}$. In other words, (4.13) was replaced with

$$w_n = w_{n-1} - \gamma J'_{\lambda, \beta}(w_{n-1}), \quad n = 1, 2, \dots \quad (6.4)$$

Note that $J'_{\lambda, \beta} \in H_0^3(R')$. This means that all functions w_n of the sequence (6.4) satisfy the same boundary conditions p_0, p_1 (2.19). We took $\gamma = 10^{-5}$ at the first step of the gradient descent method and adjusted it using line search at every subsequent iteration.

4. We choose the starting point $w_0(x, t)$ of the process (6.4) as $w_0(x, t) = -(p_1(t)x^2)/2.2 + p_1(t)x + p_0(t)$. It is easy to see that the function $w_0(x, t)$ satisfies boundary conditions (2.19) as well as boundary condition (6.1). Hence, we set at the first step of the minimization procedure

$$a_0(x) = 2(w_0)_x(x, 0) = 2p_1(0)(1 - 2x/2.2).$$

In most cases $p_1(0) = 0$, which means that the initial function $a_0(x) \equiv 0$ in most cases. Using (2.27), we set $a_n(x) = 2(w_n)_x(x, 0)$, where the function $w_n(x, t)$ is computed on the n -th step of the minimization procedure.

5. The stopping criterion for our minimization process is

$$\|a_{n+1} - a_n\|_{L^2(0,1)} / \|a_n\|_{L^2(0,1)} \leq 10^{-2}.$$

6.1. Data pre-processing and noise removal. In this section we introduce multiplicative noise to the data to simulate noise that appears in real measurements

$$u^\xi(0, t) = u(0, t)(1 + \text{rand}([- \xi, \xi])), \quad u_x^\xi(0, t) = u_x(0, t)(1 + \text{rand}([- \xi, \xi])), \quad (6.5)$$

where $\text{rand}([- \xi, \xi])$ is a random variable uniformly distributed in the interval $[- \xi, \xi]$. In all our tests we set $\xi = 0.1$, which corresponds to the 10% noise. Functions $u(0, t), u_x(0, t)$ and their noisy analogs $u^\xi(0, t), u_x^\xi(0, t)$ are depicted on Figures 2(B),(C).

The developed numerical technique requires the function $w(x, t) \in B(d, p_0, p_1)$, see (3.4) and by (2.21) functions $p_0(t), p_1(t)$ are obtained via the differentiation of the data $f_0(t)$ and $f_1(t)$. Thus, the noisy data (6.5) should be smoothed out by an appropriate procedure.

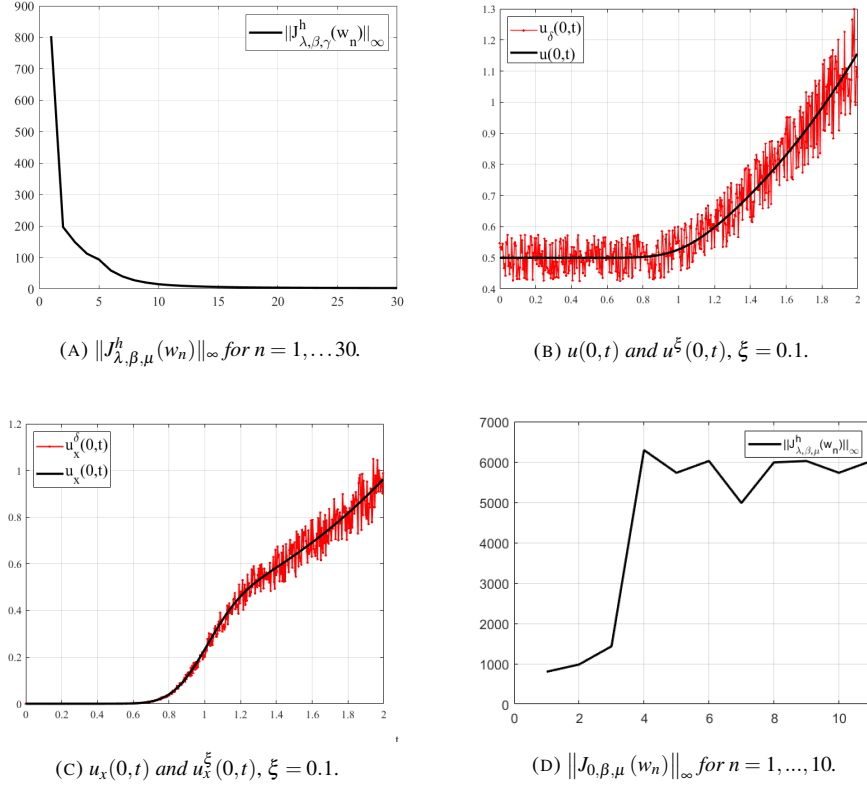


FIGURE 2. The comparison of noiseless and noisy data. Figure 2(A) shows the norm of the functional (6.2) for each iteration of the gradient descent for the test function depicted on Figure 3(A). Figure 2(D) corresponds to our test for $\lambda = 0$; see the text.

To do the latter, we use the cubic smoothing spline interpolation satisfying the following end conditions:

$$u(0,0) = 0.5, \quad u_{tt}(0,T) = 0, \quad u_x(0,0) = 0, \quad u_{xtt}(0,T) = 0.$$

Next, we differentiate so smoothed functions. Our numerical experience tells us that this procedure works quite well. Similar observations took place in all above cited works on the convexification.

6.2. Numerical results. We have calculated the relative error of the reconstruction on the final iteration $n = n^*$ of the minimization procedure:

$$\text{error} = \|a_{n^*} - a^*\|_{L^2(0,1)} / \|a^*\|_{L^2(0,1)}$$

where $a_{\text{comp}}(x) = a_{n^*}(x)$ is the computed solution and $a^*(x)$ is the true test function.

We have conducted our computations for the following four tests:

Test 1. $a(x) = x^2 e^{-(2x-1)^2}$.

The function of Test 1 is our reference function for which we have chosen the above listed parameters. We have used the same parameters in the remaining Tests 2-4.

Test 2. $a(x) = 10e^{-100(x-0.5)^2}$.

Test 3. $a(x) = 2e^{-400(x-0.3)^2} + 2e^{-200(x-0.5)^2} + 2e^{-400(x-0.7)^2}$.

Test 4. $a(x) = 1 - \sin\left(\frac{\pi(x-0.876)}{1+\pi(x-0.876)}\right)$.

Note that functions on the Figures 3(C),(D) do not attain zero values at $x = 1$ as required by condition (1.2). Also note that the function $a(x)$ in Test 4 is not differentiable at $x_0 = 0.876 - \pi^{-1} \approx 0.558$, and has infinitely many oscillations in the neighborhood of the point x_0 . Nevertheless numerical reconstructions on Figures 3(A),(D) are rather good ones, also, see Table 6.2. Graphs of exact and computed functions $a(x)$ of Tests 1-4 are presented on Figures 3 (A)-(D). Table 6.2 summarizes the results of our computations.

We have used the 12-core Intel(R) Xeon(R) CPU E5-2620 2.40GHz computer. The average computational time for tests 1-4 was 159.4 seconds with the parallelization of our code. And it was 1114.3 seconds without the parallelization. Thus, the parallelization has resulted in about 7 times faster computations.

Table 6.2. Summary of numerical results. Here $\|\cdot\|_\infty$ denotes the L_∞ norm.

Test	n^*	Error	$\ J_{\lambda,\beta,\mu}^h(w_0)\ _\infty$	$\ J_{\lambda,\beta,\mu}^h(w_{n^*})\ _\infty$
1	30	0.1628	2570	2.7465
2	33	0.2907	34.42	0.22
3	51	0.0804	3.12	0.0007
4	41	0.3222	0.82	0.0003

One can see from Table 6.2 that that the L_∞ -norm of the functional $J_{\lambda,\beta,\mu}^h$ decreases by at least the factor of 150 in all tests. The same was observed for the L_∞ -norm of the gradient of this functional (not shown in the table).

We now test some values of the parameters λ and α which are different from ones in (6.3). Below we work only with the noiseless data and with the function $a(x)$ which was used in Test 1. The parameter β below is the same as in (6.3).

First, we test values of λ which are larger and smaller than $\lambda = 2$ in (6.3). Figure 4(A) shows our result for $\lambda = 5$ and $\lambda = 1$. It is clear from Figure 4(A) that a larger value of $\lambda = 5$ provides basically the same result as the one on Figure 3(A), and both are close to the correct solution. On the other hand, the result deteriorates for a smaller value $\lambda = 1$. Next, Figure 4(B) displays our result for the limiting case of $\lambda = 0$, i.e. when the Carleman Weight Function is absent in functional (3.5). In this case the gradient descent method diverges, see Figure 2(D). Thus, we stop iterations after $n = 10$ steps. A significant deterioration of the result of Figure 4(B), as compared with Figures 3(A) and 4(A), is evident. Therefore, the presence of the CWF in (3.5) is important.

The parameter α is chosen in the interval $(0, 0.5)$. Figure 5 shows our results for two values of $\alpha = 0.2$ and $\alpha = 0.5$. Here, $\lambda = 2$, as in (6.3). One can see that both results are almost the same. A similar behavior was observed for $\alpha = 0.3$ and $\alpha = 0.4$. This shows a good stability of our method with respect to the value of α . We note that we have chosen the limiting value $\alpha = 0.5$ in our above tests in order to demonstrate that our method is robust with respect to the choice of α even if the limiting value of this parameter is chosen.

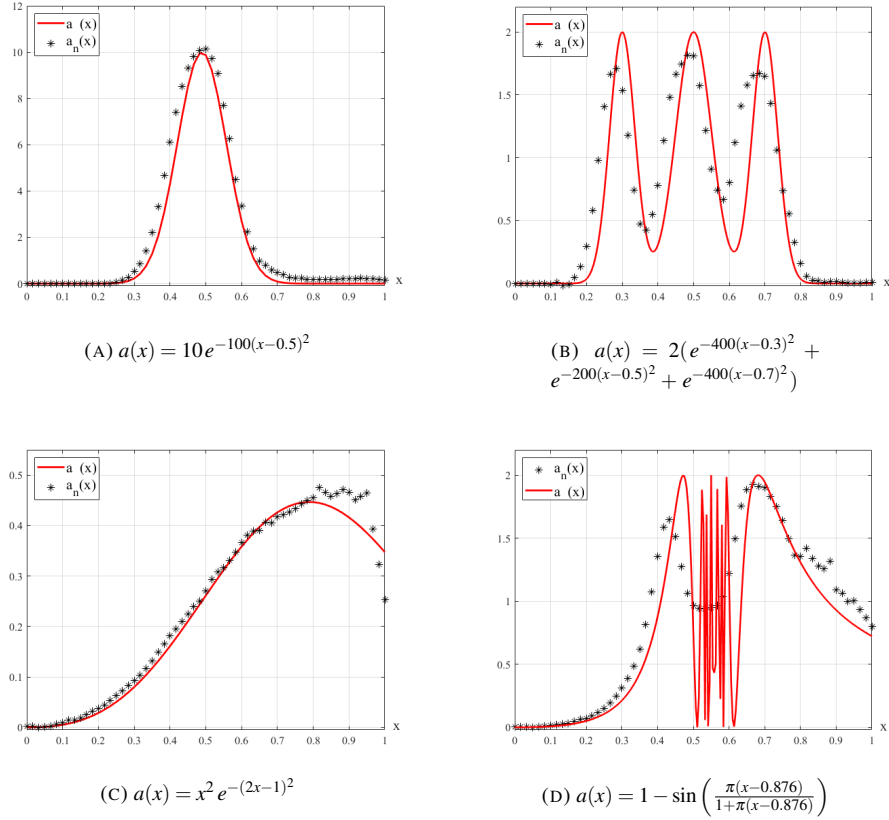


FIGURE 3. Numerical reconstructions (the black marked dots) of functions $a(x)$ (the solid lines). Noise level $\xi = 0.1$.

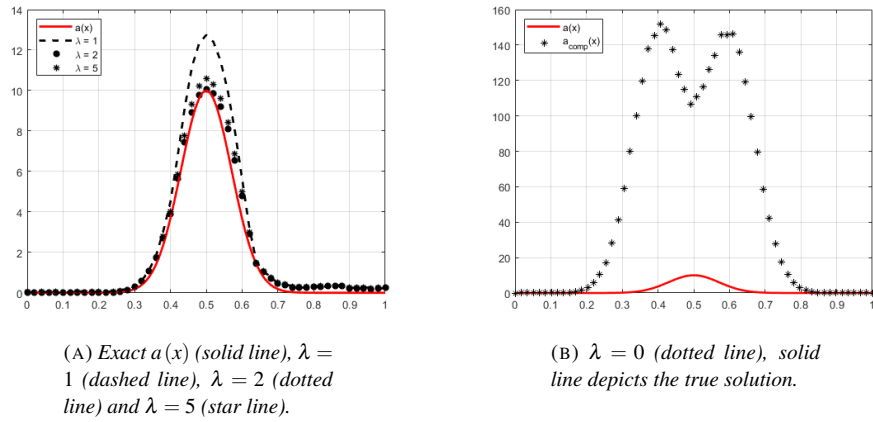
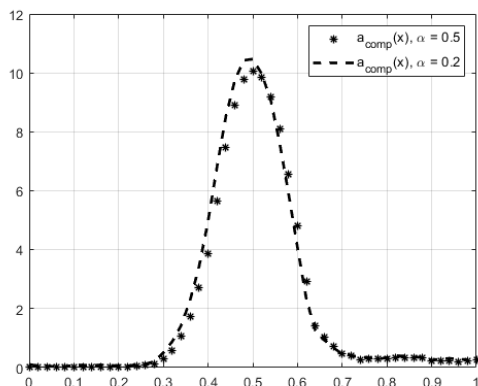


FIGURE 4. Limiting testing of different values of the parameter λ for the test function of Test 1, see comments in the text. The data are noiseless.



(A) $a_{comp}(x)$ for Test 1 with $\alpha = 0.2$ (dashed line) and $\alpha = 0.5$ (dotted line).

FIGURE 5. Testing of different values of the parameter α , see comments in the text. Solid line is the correct function of Test 1. The data are noiseless.

REFERENCES

- [1] Younes Ahajjam, Otman Aghzout, José M Catalá-Civera, Felipe Peñaranda-Foix, and Abdellah Driouach. A compact uwb sub-nanosecond pulse generator for microwave radar sensor with ringing miniaturization. In *2016 5th International Conference on Multimedia Computing and Systems (ICMCS)*, pages 497–501. IEEE, 2016.
- [2] Anatoly B Bakushinskii, Michael V Klibanov, and Nikolaj A Koshev. Carleman weight functions for a globally convergent numerical method for ill-posed cauchy problems for some quasilinear pdes. *Nonlinear Analysis: Real World Applications*, 34:201–224, 2017.
- [3] Lucie Baudouin, Maya De Buhan, and Sylvain Ervedoza. Convergent algorithm based on carleman estimates for the recovery of a potential in the wave equation. *SIAM Journal on Numerical Analysis*, 55(4):1578–1613, 2017.
- [4] Lucie Baudouin, Maya de Buhan, Sylvain Ervedoza, and Axel Osses. Carleman-based reconstruction algorithm for the waves. 2020.
- [5] Larisa Beilina and Michael V Klibanov. Globally strongly convex cost functional for a coefficient inverse problem. *Nonlinear analysis: real world applications*, 22:272–288, 2015.
- [6] Larisa Beilina and Michael Victor Klibanov. *Approximate global convergence and adaptivity for coefficient inverse problems*. Springer Science & Business Media, 2012.
- [7] Alexander L Buchgeim. Uniqueness in the large of a class of multidimensional inverse problems. In *Sov. Math. Dokl.*, volume 24, pages 244–247, 1981.
- [8] David Colton and Rainer Kress. *Inverse acoustic and electromagnetic scattering theory*, volume 93. Springer Nature, 2019.
- [9] Björn Engquist and Andrew Majda. Absorbing boundary conditions for numerical simulation of waves. *Proceedings of the National Academy of Sciences*, 74(5):1765–1766, 1977.
- [10] Izrail Moiseevich Gelfand and Boris Moiseevich Levitan. On determining a differential equation from its spectral function. *Amer. Math. Soc. Transl.*, 2(1):253–304, 1955.
- [11] Sergey I Kabanikhin, Nikita S Novikov, Ivan V Oseledets, and Maxim A Shishlenin. Fast toeplitz linear system inversion for solving two-dimensional acoustic inverse problem. *Journal of inverse and ill-posed problems*, 23(6):687–700, 2015.
- [12] Sergey I Kabanikhin, Karl K Sabelfeld, Nikita S Novikov, and Maxim A Shishlenin. Numerical solution of the multidimensional gelfand–levitan equation. *Journal of inverse and ill-posed problems*, 23(5):439–450, 2015.
- [13] Sergey I Kabanikhin, Abdigany D Satybaev, and Maxim A Shishlenin. *Direct methods of solving multidimensional inverse hyperbolic problems*, volume 48. Walter de Gruyter, 2013.

- [14] Andrey L Karchevsky, Michael V Klibanov, Lam Nguyen, Natee Pantong, and Anders Sullivan. The krein method and the globally convergent method for experimental data. *Applied Numerical Mathematics*, 74:111–127, 2013.
- [15] Vo Anh Khoa, Grant W Bidney, Michael V Klibanov, Loc H Nguyen, Lam H Nguyen, Anders J Sullivan, and Vasily N Astratov. Convexification and experimental data for a 3d inverse scattering problem with the moving point source. *arXiv preprint arXiv:2003.11513*, 2020.
- [16] Vo Anh Khoa, Michael Victor Klibanov, and Loc Hoang Nguyen. Convexification for a 3d inverse scattering problem with the moving point source. *arXiv preprint arXiv:1911.10289*, 2019.
- [17] Michael V Klibanov. Inverse problems in the large and carleman bounds. *Differential Equations*, 20(6):755–760, 1984.
- [18] Michael V Klibanov. Inverse problems and carleman estimates. *Inverse problems*, 8(4):575, 1992.
- [19] Michael V Klibanov. Global convexity in a three-dimensional inverse acoustic problem. *SIAM Journal on Mathematical Analysis*, 28(6):1371–1388, 1997.
- [20] Michael V Klibanov. Carleman estimates for global uniqueness, stability and numerical methods for coefficient inverse problems. *Journal of Inverse and Ill-Posed Problems*, 21(4):477–560, 2013.
- [21] Michael V Klibanov and Olga V Ioussoupova. Uniform strict convexity of a cost functional for three-dimensional inverse scattering problem. *SIAM Journal on Mathematical Analysis*, 26(1):147–179, 1995.
- [22] Michael V Klibanov and Vladimir G Kamburg. Globally strictly convex cost functional for an inverse parabolic problem. *Mathematical Methods in the Applied Sciences*, 39(4):930–940, 2016.
- [23] Michael V Klibanov, Aleksandr E Kolesov, and Dinh-Liem Nguyen. Convexification method for an inverse scattering problem and its performance for experimental backscatter data for buried targets. *SIAM Journal on Imaging Sciences*, 12(1):576–603, 2019.
- [24] Michael V Klibanov, Aleksandr E Kolesov, Anders Sullivan, and Lam Nguyen. A new version of the convexification method for a 1d coefficient inverse problem with experimental data. *Inverse Problems*, 34(11):115014, 2018.
- [25] Michael V Klibanov, Andrey V Kuzhuget, Sergey I Kabanikhin, and Dmitriy V Nechaev. A new version of the quasi-reversibility method for the thermoacoustic tomography and a coefficient inverse problem. *Applicable Analysis*, 87(10-11):1227–1254, 2008.
- [26] Michael V Klibanov, Jingzhi Li, and Wenlong Zhang. Convexification for the inversion of a time dependent wave front in a heterogeneous medium. *SIAM Journal on Applied Mathematics*, 79(5):1722–1747, 2019.
- [27] Michael V Klibanov, Jingzhi Li, and Wenlong Zhang. Convexification of electrical impedance tomography with restricted dirichlet-to-neumann map data. *Inverse Problems*, 2019.
- [28] Michael V Klibanov, Jingzhi Li, and Wenlong Zhang. Convexification for an inverse parabolic problem. *arXiv preprint arXiv:2001.01880*, 2020.
- [29] Jussi Korpela, Matti Lassas, and Lauri Oksanen. Regularization strategy for an inverse problem for a 1+ 1 dimensional wave equation. *Inverse Problems*, 32(6):065001, 2016.
- [30] Jussi Korpela, Matti Lassas, and Lauri Oksanen. Discrete regularization and convergence of the inverse problem for 1+ 1 dimensional wave equation. *arXiv preprint arXiv:1803.10541*, 2018.
- [31] Mark G Krein. On a method of effective solution of an inverse boundary problem. In *Dokl. Akad. Nauk SSSR*, volume 94, pages 987–990, 1954.
- [32] Andrey V Kuzhuget, Larisa Beilina, Michael V Klibanov, Anders Sullivan, Lam Nguyen, Michael A Fiddy, ARL Team, et al. Blind backscattering experimental data collected in the field and an approximately globally convergent inverse algorithm. *Inverse Problems*, 28(9):095007, 2012.
- [33] Boris T Polyak. Introduction to optimization. optimization software. *Inc., Publications Division, New York*, 1, 1987.
- [34] Vladimir G Romanov. *Inverse problems of mathematical physics*. Walter de Gruyter GmbH & Co KG, 2018.
- [35] John A Scales, Martin L Smith, and Terri L Fischer. Global optimization methods for multimodal inverse problems. *Journal of Computational Physics*, 103(2):258–268, 1992.
- [36] Andrei N Tikhonov, A Goncharsky, V Stepanov, and Anatoly G Yagola. *Numerical methods for the solution of ill-posed problems*, volume 328. Springer Science & Business Media, 2013.

Received xxxx 20xx; revised xxxx 20xx.

E-mail address: smirnov.phd@gmail.com

E-mail address: mklibanv@uncc.edu

E-mail address: loc.nguyen@uncc.edu